TRANSACTIONS OF THE INSTITUTE OF AVIATION
No. 4 (245), pp. 87-102, Warsaw 2016
DOI: 10.5604/05096669.1226428

ISSN 0509-6669
eISSN 2300-5408

NUMERICAL ANALYSIS AND OPTIMIZATION OF MOTOGLIDER'S PROPELLER STRUCTURE

Mateusz Lis

Institute of Aviation, Al. Krakowska 110/114, 02-256 Warsaw, Poland
matlis1@op.pl

Abstract

The purpose of this paper is to present numerical analysis methodology and structural optimization process of composite propeller intended to be used in propulsion unit of an AOS-71 motoglider. The main objective is to minimize the propeller's weight which is always desirable in aviation and additionally reduce materials usage which effects the total costs. At the beginning of the paper, some general information is presented about requirements that propeller should meet. Afterwards, basic propeller technical data and its work conditions are shown. The main part of this paper focuses on all steps undertaken to get the final result which are 3D model creation including some simplifying assumptions in terms of propeller geometry, FEM mesh model construction that reflects structural layout and physical properties of the real object accurately enough and after that, preparations for numerical analysis and computation process itself in ANSYS software. The final outcome of the paper presents results from the analyses and discussion about usefulness of the process and conclusions in the future propellers constructions.
Keywords: numerical optimization, composite structures, FEM, motoglider propeller.

1. INTRODUCTION

Propeller is a mechanism that converts rotational motion into thrust. It has been used since the early days of aviation and despite rapid development of jet engines, it is continuously developed. Due to its relative simplicity, it is widely used in general aviation and sports aeroplanes, motogliders, ultralights and paragliders but also in much larger aeroplanes such as regional airliners and military transport aeroplanes. Throughout the years, together with aeroplane materials and technology development, propellers design and manufacturing techniques evolved as well. Nowadays, composite materials and advanced manufacturing processed are common in propellers production.

The propeller which is the object of the analysis is supposed to be used in an experimental AOS-71 motoglider propulsion unit. It is a constant pitch propeller driven by brushless synchronous motor A37K015 with output power of 30 kW at 1900 rpm. The AOS-71 motoglider as well as it propeller presented in figure 1 have been designed in cooperation between Warsaw University of Technology and Rzeszow University of Technology while the propeller structure has been fully designed and manufactured in the former one.

Fig. 1. AOS-71 motoglider during flight tests [1]

Due to specific propeller work conditions, following crucial factors should be taken into account to make sure of its airworthiness and safety:

- High strength and stiffness resulting in good vibration resistance;
- High fatigue limit;
- Resistance to erosion and damage in the case of foreign object impact;
- Lightweight and correct balancing;
- External surface smoothness and high fidelity of geometry that impact aerodynamic efficiency;
- Pitch change mechanism reliability and low power consumption;
- Easy maintenance and disassembly, repeatability of components, especially blades.

Except for those obvious points, more precise requirements are covered in JAR-P regulations, where the most important ones for the case covered in this paper are listed below. All of them have been used in the analyses shown further:

- JAR-P 170 - specifies centrifugal loads trials;
- JAR-P 180 - specifies flutter check requirements;
- ACJ-P 60 - covers requirements for acceptable static loads level in propeller components.

As stated previously, this paper will focus on optimization of the propeller structure. Description of typical methodology, assumptions and advantages of the numerical composite structures optimization can be found in [2]. From the mathematical point of view, optimization is a process whose purpose is to maximize (or minimize) a real function that describes key object properties by iterative choosing of input values within an allowed domain and computing a value of this function every time taking into account different constraints set for the solution. Technically, it can be described by graph as shown in figure 2 that presents typical phases of optimization process and data flow. This kind of graph can be applied for optimization in different technical areas, not only structural as described below. First of all, at the beginning of the analysis, technical problem should be defined and modelled. That is crucial to provide rough estimates of input values correctly because it allows to save computation time and reduce the risk that the process may miss the best solution as optimization algorithms are often very vulnerable to wrong initial conditions. After that, analysis is performed for given conditions (loads, constraints, etc.) and the received solution is checked, manually or in the case of automatic processes, by definition of objective function that indirectly describes results quality and usefulness. Providing the results are satisfactory, the process can be finished or repeated until expected results are achieved. In the case the results are not satisfactory, a project is slightly modified, and then analysis and evaluation process starts again. The “amount”

and "direction" of change depends on the algorithm type, user predefined preferences and also variables type and quantity. Those are the key factors in an efficient optimization process that cannot be generalized but have to be adjusted to every analysis separately. An optimization process is repeated iteratively and usually stops when a satisfactory result is achieved or the maximum number of iterations is exceeded. Regardless of the reason, the outcome ought to be evaluated manually and then the human expertise matters much in the final assessment.

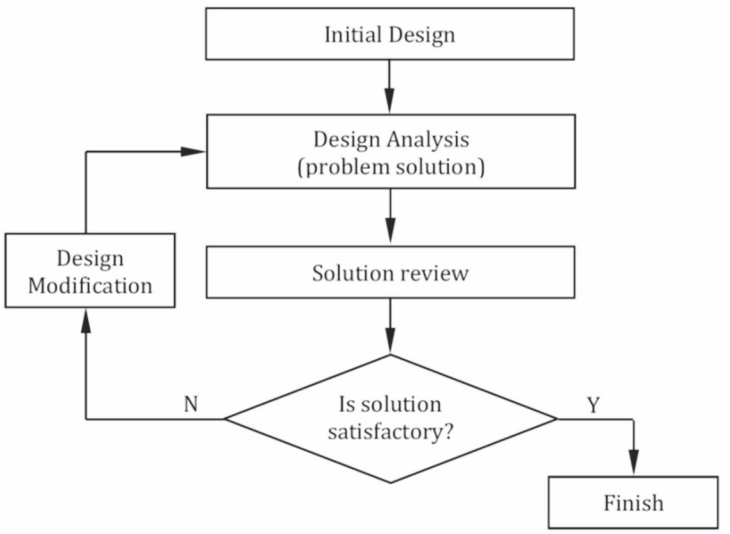

Fig. 2. General scheme of optimization process [Lis, 2016]

2. PROPELLER DESCRIPTION

Before any analyses can be performed, it is essential to familiarize with the real propeller structure and to collect any required technical data. A propeller is generally made of carbon-epoxy composite with minor use of glass fabrics. As shown in figure 3a below, both two blades are single monolithic part, manufactured simultaneously. Blades are mounted into three-piece composite hub (see figure 3b) and all assembly components are connected together using epoxy adhesive. After the curing process, with the use of six bolts, assembly is connected to aluminum disc that transmits torque from the motor shaft.

Because the propeller is periodically symmetric, unless otherwise stated, further analyses will be performed for a single blade (one half of the propeller). There are following structural and manufacturing components shown in figure 4 that can be derived from the blade structure:

- Main spar, transmitting normal and centrifugal (mass) loads. It is made mostly of unidirectional carbon fabric (SGL KDU 1007);
- Top and bottom skin, transmitting torsion moment. It is made of three layers of symmetric bidirectional carbon fabric (ECC 447) placed in the negative mold and vacuum-cured;
- Three foams, which fill the gap between skins and spar preventing skins from buckling. Made of expanding, epoxy-based adhesive (RENCAST CW2215);
- Three layers of symmetric bidirectional carbon fabric (ECC 447) whose purpose is to integrate all components together and support skins in shear loads transmission.

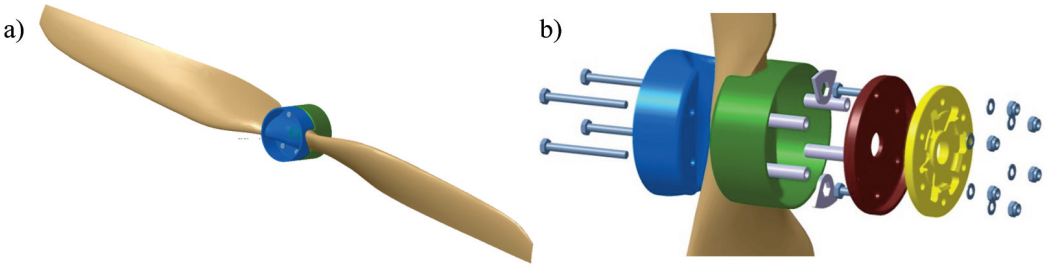

Fig. 3. a) General view of the propeller; b) Hub components and blades installation into the hub [Lis, 2016]

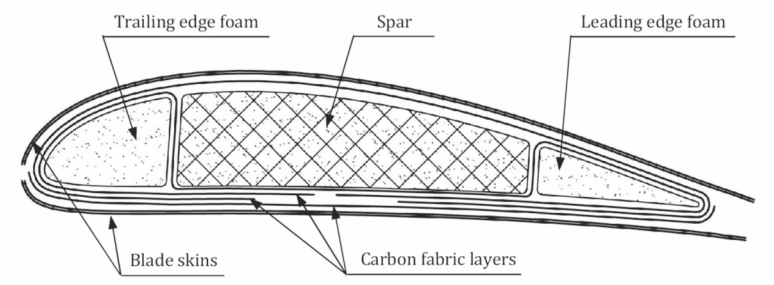

Fig. 4. Blade cross-section showing internal structure [Lis, 2016]

Because of its complexity and ingenuity at once, spar structure requires a separate description. As shown in figure 5, beginning from the inside, it consists of the following structural components:

- Inner foam, molded separately (RENCAST CW2215);
- Single (short) layer of bidirectional carbon braid (120.14472226-C);
- Inner ring, carbon roving;
- Single (long) layer of bidirectional carbon braid (120.14472226-C);
- Spar main skin; one layer of bidirectional glass fabric (Interglass 92125) and number of unidirectional carbon fabrics. Number of carbon layers varies with the blade length from 10 on the root to 5 on the tip;
- Single (short) layer of bidirectional carbon braid (120.14472226-C).

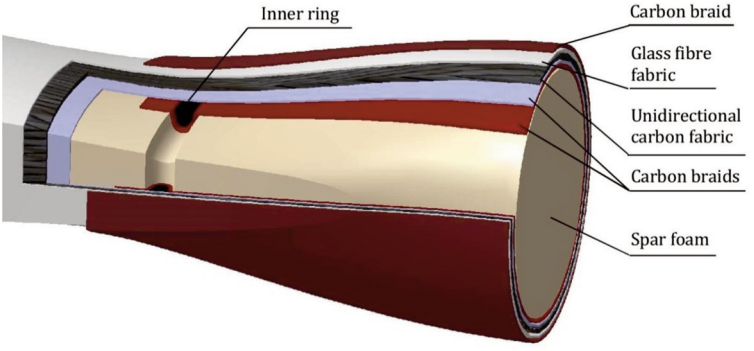

Fig. 5. Spar internal structure [Lis, 2016]

Mechanical properties of the materials used in propeller construction are presented in table 1. Because of the fact that this data is very seldom available, it has been mostly defined as stated in [3]

based on the experimental data described in [4]. Determination of composite properties on the basis of experimental data received in specific workshop is recommended as it strongly depends on environmental conditions, staff experience, tooling used, and moreover, mechanical properties deteriorates with time [5, 6].

Tab. 1. Mechanical properties of fabrics and expanding foam used for blade manufacture [3]

	$\bar{m}$	δ	R_m	R_c	E_x	E_y	E_z	G_{xy}	G_{yz}	G_{zx}	ν_{xy}	ν_{yz}	ν_{xz}
	g/m^2	mm	MPa								-		
ECC 447	160	0.18	545	510	51830	51830	9890	18730	3200	3200	0.04	0.26	0.26
SGL KDU 1007	200	0.15	1000	660	90000	9890	9890	5300	3200	3200	0.19	0.3	0.26
120.14472226-C	154	0.17	545	510	51830	51830	9890	18730	3200	3200	0.04	0.26	0.26
Interglass 92125	280	0.26	302	295	19360	19360	12760	7230	4060	4060	0.05	0.35	0.35
Rencast CW 225 +REN HY5161 +DY 5054	-	-	1.55	0.75	55			22			0.25		

3. NUMERICAL MODEL CREATION

This chapter describes phases of numerical model preparation and assumptions set on every step. That was especially important part of work since its purpose was to describe real object as a numerically correct and computable model that will reflect the reality accurately enough but, on the other hand, will not be very complex and computationally expensive. Numerical analysis methodology and design issues related to the composite structures similar to presented herein can be also found in [7, 8, 9].

3.1. 3D model creation

Geometrical model was created in CATIA V5R18 software based on the external blade surface. After some corrections that were mainly smoothness improvements, a target model could be created. The geometrical model was split into 26 components, out of which 7 were solid components reflecting expanding foam and the others were surface components supposed to be layered composite components. This way of division was driven mainly by differences in internal structure of blade, but also manufacturing and model clarity aspects were taken into account [10]. There are following components derived in the model:

- Spar foams (fig. 6). In reality, it is single component but in the model, because of the inner carbon ring (see fig. 4), it was split into three parts, where the foam 2 is the insert that copies the ring properties. This foam will have modified mechanical properties to imitate ring stiffness;
- Spar shells (fig. 7). The spar main structure was divided into 7 segments according to actual layout of unidirectional fabric and braids (see fig. 5);
- Foams (fig. 8). Component Inner foam imitates expanding glue on connection between spar and blade skins. The remaining ones are produced at earlier stages as separate parts.
- Inner walls (fig. 9). Those are created by fabric layers integrating blade components (see fig. 4), connect to both blade skins and take part in normal (shear) loads transfer;
- Top and bottom skins (fig. 10). Divided into five segments each, which comes from layout differentiation because of integrating fabric layers (see fig. 4).

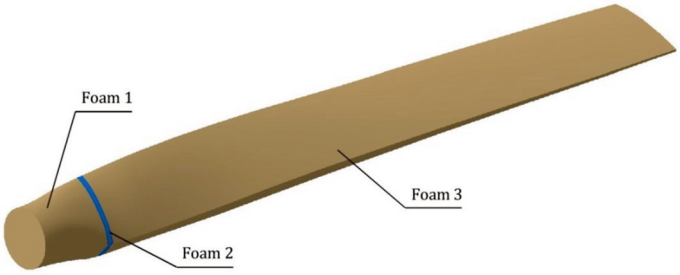

Fig. 6. Spar foams [Lis, 2016]

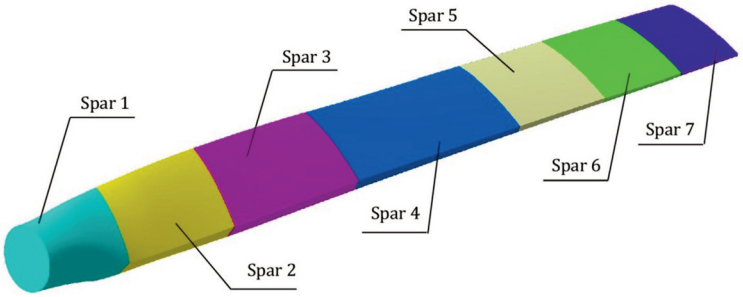

Fig. 7. Spar shells division [Lis, 2016]

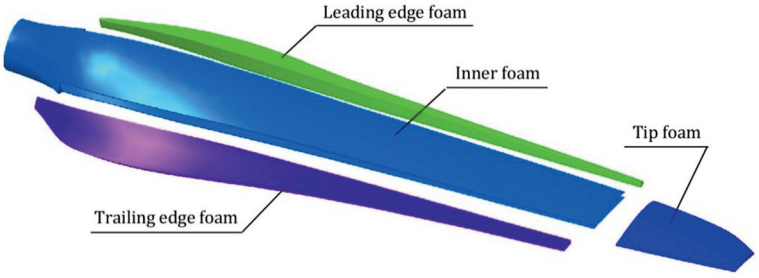

Fig. 8. Inner foams [Lis, 2016]

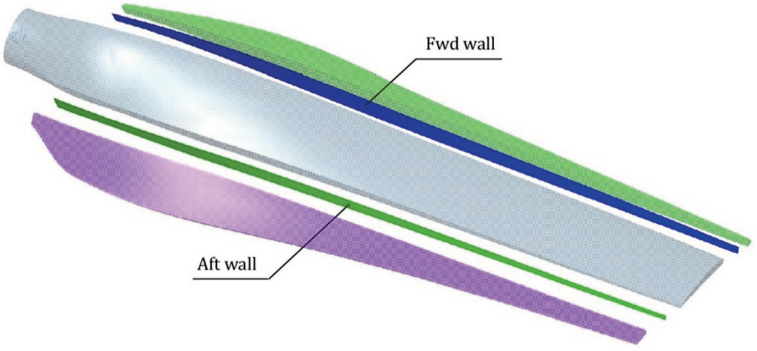

Fig. 9. Inner walls [Lis, 2016]

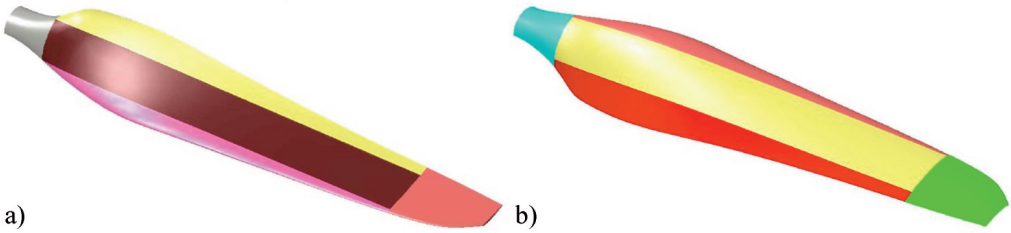

Fig. 10. Blade skins: a) bottom; b) top [Lis, 2016]

3.2. Mesh model creation

Geometrical model described above was used to build mesh model in HyperMesh 10.0 software [11]. Except for geometry modification, this software enables element type, Real Constant and material properties definition as well as many other useful operations. Because of the complex blade shape and curvatures, it was decided that mesh will inherit second order elements that much better reflects high curvature shapes [12, 13]: triangle SHELL91 in case of shell and tetrahedral SOLID95 elements for solid components. While creating the mesh, local element coordinate systems have been defined according to real structure, technology of manufacturing and the way of model construction. The mesh is described by surfaces with nodes lying on it and the direction of element normal vector as shown in figure 11 and figure 12.

One of the requirements in hybrid mesh check is that every node of shell element is coincident with adjacent node of solid element limited with the same surface, i.e. there is no offset considering shell elements thickness. That means in mesh model some shell elements will interfere with solid elements, which in reality is impossible. From this reason, in order to avoid differences in mass and thus, centrifugal forces, density of shell components defined by *Real Constant* was reduced by foam density in each case where applicable. As a result, there were 12 different *Real Constants* created and eventually applied to appropriate components.

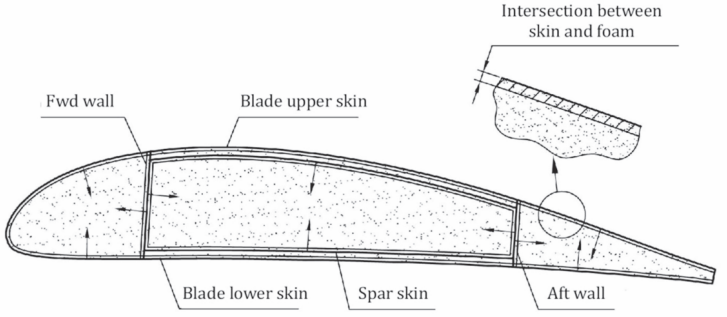

Fig. 11. Normal directions of the surfaces in mesh model [Lis, 2016]

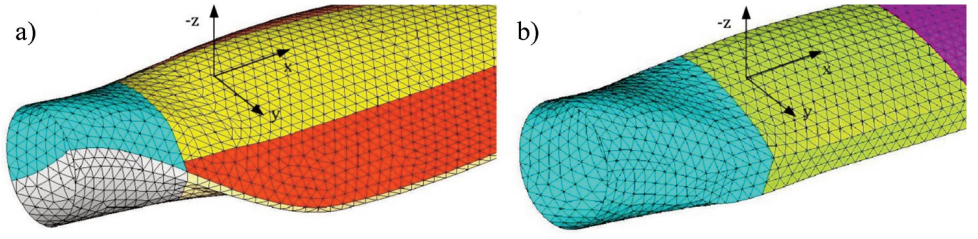

Fig. 12. Local element coordinates systems in: a) blade skin; b) spar skin [Lis, 2016]

Tab. 2. List of parameters defining number of layers in spar sections [3]

Spar section	Parameter	Value
spar_1	t_1	10
spar_2	t_2	10
spar_3	t_3	9
spar_4	t_4	8
spar_5	t_5	7
spar_6	t_6	6
spar_7	t_7	5

The final definition of Real Constants for spar section components (see fig. 6) was made in ANSYS software with the use of parameters describing the number of unidirectional fabrics in each of the component as shown in table 2. Because none of the unidirectional fabric layer (SGL KDU 1007) in each section was separated by another type of fabric, the bunch of layers could be modelled as a single one using Real Constant with total thickness equal to single layer thickness δ (table 1) multiplied by the number of layers t_i (table 2). This parametrization was essential due to optimization process specification that will be explained further.

4. NUMERICAL ANALYSIS AND OPTIMIZATION PROCESS

Before an analysis can be started, some preparations are required. Those are definitions of boundary conditions, loads and validation of the model. It should be done with significant care, as it impacts directly final results if any mistakes or excessive simplifications have been assumed.

4.1. Boundary conditions and loads

As stated before, blades are mounted into two-piece composite hub and all components are bonded together. This defines the way that boundary conditions are applied. It is shown in figure 13a and generally consists of periodic symmetry constraint on nodes lying on the XY plane and displacement constraint in the area marked in yellow.

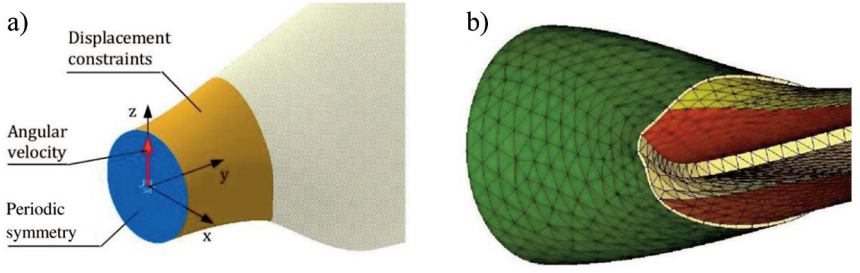

Fig. 13. a) Boundary conditions on blade root; b) additional bonding layers on blade root [Lis, 2016]

Because the blade root is not fixed ideally rigidly in the hub and so that it would not be sufficient to fix nodes on the blade, additional bonding layer of 1mm thickness and 70mm width (hub diameter equals 140 mm) has been modelled as shown in figure 13b. There is also an additional shell layer outside whose nodes are fixed in all translations directions. This solution seems to be most adequate in this case as it does not fix nodes rigidly, which is not present in a real object.

There are two loads acting on the blade when it operates: inertial loads (centrifugal) and aerodynamic loads. Inertial loads are modelled in ANSYS by definition of revolution speed of appropriate value and in adequate coordinates system. After considering applicable JAR-P requirements, which states that propeller should take inertia loads twice larger as nominal, revolution speed would be then:

$$\omega_{\max} = \frac{2\pi \cdot n_{nom} \cdot \sqrt{2}}{60} = 280\, rad/s \quad (1)$$

where: n_{nom}=1900 rpm.

Aerodynamic loads were computed in FLUENT software as stated in [14]. Description of aerodynamic analysis methodology is not presented herein as it is out of the scope of this paper so that only general information and assumptions are presented. Thorough description of the computational fluid mechanics analyses approaches, assumptions required and results discussions for various propellers types can be found in [15, 16, 17, 18].

In the scope of this paper, following boundary conditions and solver settings have been defined:

- *Pressure far field* – condition of far field on the perimeter, front and aft wall of the half-cylinder field being analyzed, undisturbed flow in far field;
- *Wall* – condition that defines boundary between solid object and fluid, for viscous flow essential to be defined in order to simulate boundary layer correctly;
- *Periodic interface* – condition that includes into analysis second half of the flow field;
- *Spalart-Allmaras* turbulence model;
- Gas parameters:
  - specific heat: 1006.43 J/kgK;
  - thermal conductivity: 0.0242 W/mK;
  - dynamic viscosity: $1.7894 \cdot 10^{-5}$ Pa·s;
- Revolution speed: 280 rad/s;
- Flight speed: 0 m/s

The simulation was performed for static conditions, which means there was no linear flight velocity modelled. This case was defined because together with factored revolution speed it generates the highest possible loads. A result of aerodynamic computation was a map of pressure on blade surface. It was imported into ANSYS model and after interpolation to different mesh, was applied to model as a set of forces acting on nodes placed on blade outer surfaces.

4.2. Model validation and preliminary calculations

A purpose of the preliminary calculations is to check whether the numerical model was defined correctly, i.e. whether the mesh, boundary conditions and loads reflect the reality accurately enough. The easiest way to do this is to apply loads, whose effect is known or easy to predict or calculate. Therefore, two different calculations were carried out.

The first one was a determination of reaction loads without aerodynamic pressure on the blade surface. Inertial loads are the only ones acting on the blade, so that reaction F_y should be equal to theoretical centrifugal force:

$$F_c = \omega_{\max}^2 \cdot y_c \quad (2)$$

where: m=1.328 kg – blade weight, y_c=0.335 m – blade center of gravity position.

These two values have been defined according to data generated automatically by ANSYS software. During the second analysis reactions F_x, F_y, F_z have been determined based on the aerodynamic loads only applied on blade surface. In this case, reference reaction forces were determined according to data from FLUENT. Results received from analyses and their comparisons are presented in table 3 below.

Tab. 3. Model validation results [3]

	Reaction force [N]	Reference value [N]	Computed value [N]	Error [%]
Analysis 1	F_x	-	-	-
	F_y	34878.59	34890.32	0.034
	F_z	-	-	-
Analysis 2	F_x	799.28	787.95	-1.42
	F_y	-96.63	-87.79	-9.15
	F_z	1894.45	1888.,22	-0.33

As it can be easily seen, that for the first analysis there was a nonsignificant difference in reaction force of about 0.03%. The biggest error occurred in second analysis, where the F_y force deviation reached over 9% of reference value. Such significant relative deviation may come from pressure interpolation error when transferring forces from mesh used in aerodynamic calculations to nodes of elements used in structural analysis. Nevertheless, the difference of 11 N in aerodynamic force seems to be insignificantly low in comparison to 36 kN of inertial load. The remaining reaction forces deviations are very small, therefore it can be said that numeric model was created properly and can be used in further analyses.

Tab. 4. Natural oscillation frequencies of blade [3]

Mode	Frequency [rad/s]
1	245
2	279
3	322
4	384
5	463

According to JAR-P regulations, additional analysis was performed to check natural oscillations frequencies for several modes. It was assumed that none of the modes can occur within range of $0 – 1.1\omega_{nom}$, which means it should be greater than 220 rad/s. Similarly to previous analyses, appropriate boundary conditions were applied, revolution speed of 220 rad/s and aerodynamic loads either. However, contrary to the previous analyses, full propeller was analyzed to cover nonsymmetrical oscillation modes. Additionally, because of the loads possessed were calculated for ω_{max} = 280 rad/s, it was essential to recalculate it for ω_{max} = 220 rad/s. It was done with a simple assumption that aerodynamic forces are proportional to $\sqrt{\omega}$. Results of calculation are presented in table 4, which shows natural oscillation frequencies for the first five oscillation modes. The lowest of computed oscillation frequencies is higher than the assumed maximum revolution speed, which means there is no possibility to induce self-oscillation in the assumed conditions. Because of that, it is not necessary to perform stress analyses for self-oscillation cases. Detailed description of the issues related with airplanes structures vibrations and methods of analysis are described in [19, 20].

4.3. Optimization process

Preparation for numerical optimization begins with the definition of some variables and parameters that defines the problem, its possible solution domain and constraints. Therefore, a set of *Design Variables*, *State Variables* and the *Objective* function were defined.

Design Variables are parameters that describe the number of unidirectional carbon fiber layers in spar sections (see figure 7 and table 5). These are parameters that are to be changed by numerical algorithm in search for the best solution. Ideally, these parameters should be integer type (as defines the number of layers), however, in this analysis they are real type to simplify the question. Without this assumption, the *Objective* would be discontinuous function, then the gradient or interpolation search algorithms are ineffective, which means that it would be very difficult, if not impossible, to

achieve a satisfactory solution. According to the information given previously (tab. 2) minimum, nominal and maximum value of each *Design Variable* were defined as shown in table 5. Those values specify allowed domain of *Design Variable*. The maximum difference between variables in successive iterations was set as default to 1% of difference between maximum and minimum value.

Tab. 5. Design Variables domain definition [3]

Design Variable	Minimum	Maximum	Nominal
t_1	4	10	10
t_2	3	10	10
t_3	2	9	9
t_4	1	8	8
t_5	0.5	7	7
t_6	0.2	6	6
t_7	0.1	5	5

State Variables are quantities that constrain the design, i.e. define the domain of permissible solutions. Dependently on the problem complicity, there can be one or more of them. In structural analyses they are usually maximum load, stress or strain values. In the current analysis, all *State Variables* are defined as maximum tension stress in unidirectional layers of spar components. After preliminary analyses it appeared that compression stress is significantly lower and does not constrain the structure. Therefore, it was decided not to add *State Variables* for compression as every additional parameter considerably increases analysis costs. Similarly, stress in other components of blade was checked and did not seem to be critical in any location. Similarly to the *Design Variables*, minimum, maximum and tolerance for *State Variables* were defined. The minimum value was set to 0 in every case and tolerance as default to 1% of the maximum value. The maximum values were defined according to ultimate stress for material divided by an appropriate factor that changes from 2 on the root to 1.75 on the blade tip as stated in JAR ACJ-P 60. Results are presented in table 6.

Tab. 6. State Variables domain definition [3]

State Variable	Minimum [MPa]	Maximum [MPa]
σ_{x1}	0	500
σ_{x2}	0	510
σ_{x3}	0	522
σ_{x4}	0	538
σ_{x5}	0	553
σ_{x6}	0	563
σ_{x7}	0	571

Objective Function is the function dependent on *Design Variables* that is to be minimized. In this case it was defined to be a sum of all spar shell elements volumes, which means it reflects directly spar weight and thus, impacts the mass of the whole propeller. Tolerance for *Objective Function* was left as default 1%. This value describes the maximum allowed change of *Objective Function* between two succeeding iterations. Small values are advised for nonlinear problems because the method of small steps is efficient in such cases, however, too small tolerance can significantly increase the

number of iterations and computation time. Out of two major optimization methods available in ANSYS [21]: *Subproblem approximation* and *First order*, the former one was chosen. It is an advanced zero-order method, which uses values of *Objective Function* and some other functions dependent on *Design Variables* but does not use derivatives. For random values of *Design Variables* it creates approximation of *Objective Function* and *State Variables*, which are used to search for a new set of *Design Variables*. After those preparations had been finished, the first optimization was launched. During the computation process, propeller motion in all degrees of freedom was fixed as shown in figure 13b. Main aerodynamic loads were applied and centrifugal force was simulated by definition of respective revolution speed according to paragraph 4.1. The first stage of optimization process stopped after 19 iterations as from the mathematical point of view, solution has been found. Evolution of *Objective Function* values throughout this analysis can be found in figure 14. Despite the *Objective Function* was reduced almost twice, brief review of the results revealed that the optimal solution was not found. First of all, it was because the *Objective Function* values varied significantly in successive iterations rather than progressively nearing to the constant minimal value. Secondly, the Design Variables did not get the expected values and therefore, the achieved *State Variables* were not close enough (that is actually expected when performing structural optimization) but mostly far below and one of them above the maximum permitted value. This situation was caused by too high default tolerances (that equal 1% of variable range, see tab. 5) for of *Design Variables*, which resulted in premature solution convergence. To solve this issue, values of input parameters were reduced to (all of them are absolute values):

- Design Variables: 0.01;
- State Variables: 1;
- Objective Function: 10.

After this redefinition, second optimization process was launched. Again, after 19 iterations analyses stopped (see fig. 14). Results received that time were much better but still not satisfactory as *State Variables* in spar sections number 6 and 7 were far below the expected values which can be explained by high resultant *Design Variables* in these locations. To cope with this issue, four additional sets of *Design Variables* were defined manually and calculated. That was to manually "force" algorithm to change the area of search. Results showed that only one of them was not acceptable because of excessive tension load in section number 5, so that the remaining three were added to the set of possible solutions.

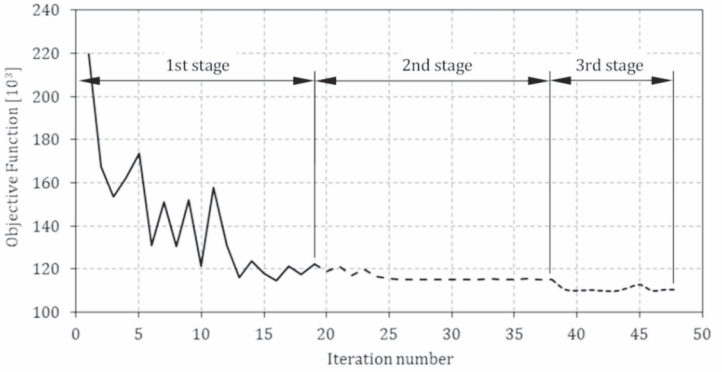

Fig. 14. Objective function value versus iteration number [Lis, 2016]

After that, the third calculation was started that lasted only 6 iterations but opposite to the previous ones, this time results were satisfactory and rational. The results of optimization in terms of *Objective*

Function value are presented in figure 14. Reduction of 49.7% in quantity of unidirectional carbon fabrics seems to be a good result as it gives an opportunity to reduce weight of the whole propeller. As it can be easily predicted, final values of *Design Variables* received from the analysis were not integer but real type numbers. It is presented in table 7 together with the resulting *State Variables*.

Tab. 7. Final numerical optimization results [3]

Design Variable		State Variable [MPa]	
t_1	4.43	σ_{x1}	498.95
t_2	6.3	σ_{x2}	508.04
t_3	2.99	σ_{x3}	504.78
t_4	1.82	σ_{x4}	538.09
t_5	0.91	σ_{x5}	551.72
t_6	0.21	σ_{x6}	539.69
t_7	0.11	σ_{x7}	309.25

4.4 Results analysis and discussion

Due to the fact that the number of layers in spar was optimized, it could not be left as received but rounded up to make the design feasible. That meant the solution could have been upset due to the change in spar stiffness and mass distribution. For this reason, single computation has been performed to check whether there are any locations with stress areas above the allowed limits. As a result, new values of *State Variables* were retrieved as shown in table 8.

Tab. 8. Optimization final results after corrections [3]

Design Variable		State Variable [MPa]	
t_1	7	σ_{x1}	361.75
t_2	7	σ_{x2}	475.87
t_3	3	σ_{x3}	510.29
t_4	2	σ_{x4}	510.25
t_5	1	σ_{x5}	538.91
t_6	1	σ_{x6}	350.17
t_7	1	σ_{x7}	223.51

As shown in the table above, none of the *State Variables* has exceeded the limit, which means the design is acceptable and can be treated as final. For certainty, stress distribution in all blade components has been reviewed with positive results but due to limited space of this paper, only stress distribution in spar unidirectional carbon layer are presented below in figure 15a and figure 15b. For detailed information about structural loads in the remaining components please refer to [3].

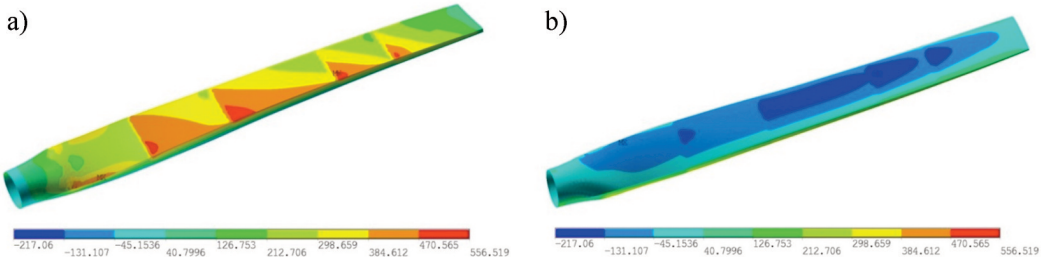

Fig. 15. a) σ_x stress distribution in the a) lower and b) upper spar surface [3]

After a review of those basic results, it was visible that there were possibilities of additional modifications that could improve the design further. The first modification proposal was to make chamfering on spar layers. The idea was to adjust layers shape on the ends to the stress map presented in figure 15 by red and yellow colors. Except for weight and costs reduction, this solution is supposed to be beneficial in terms of stress concentration. Chamfering would make spar stiffness distribution across the blade length smoother, which means stress distribution should become smoother as well.

The other proposal is to use grammage of carbon fabric for spar skin twice lower. The main advantage of this solution comes from the fact that during the facilitation of numerical results, numbers from table 7 would have to be doubled and then rounded up, which in consequence should lead to material saving in weight. Unfortunately, fabric prize is not linearly proportional to its grammage, so that the cost saving would not be probably so significant. However, this solution seems to be beneficial, too. Based on the available results, weight and costs savings were estimated for the basic solution and its two modifications described above and shown in table 9.

Tab. 9. Comparison of weight and costs of propeller for various spar layouts [3, 22]

	Weight		Cost	
	[g]	[%]	[PLN]	[%]
Baseline structure	2656	100	715	100
Optimal solution	2452	92.3	529	74
Optimal solution +layers chamfering	2437	91.8	504	71
Reduced grammage	2444	92.0	578	81

As is apparent from the table above, it is possible to reduce the propeller weight up to 8%, which seems to be a good result. It looks even more promising in terms of costs, because calculations revealed a possibility of 29% cost reduction if optimal solution is applied together with layers chamfering. However, it is worth pointing out that the cost of expanding epoxy foam is not taken into account in those calculations as it is difficult to predict. Contrary to the predictions, cost reduction in the case when a twice lower grammage fabric is used, is not as high as it was supposed to be. This is because of high price that is not proportional to grammage. Nevertheless, it gives weight reduction similar to the previous solutions and can be even better if chamfering is introduced.

5. CONCLUSIONS

The research presented in the paper aimed at optimization of propeller structure by modification of spar design. Available software for mechanical design and stress analysis was used to perform analyses that proved law regulations and stress requirements are satisfied. In order to perform the work although there are no regulations pointing composite propellers, JAR-P regulations were used to define basic requirements for the propeller structure. One of the most crucial elements of the research was preparation of numerical model to be analyzed. It was a difficult task, as always is a compromise between a model simplicity and its fidelity, which in result affects final results credibility. There were several minor changes to the mesh shape to improve its quality and to eliminate locations of stress concentrations. Some issues arose from the real blade construction, i.e. a thin layer of bonding foam between spar and blade skins was problematic to mesh as comparing to the other directions of the element, this one was crucial and caused that some mesh quality checks were not passed. Finally, the fourth version of FEM mesh was found to be correct and used in the analyses. With the use of ADPL macro and functionalities of ANSYS software, three-stage optimization process was performed the results of which was a theoretical structure of spar skin and respondent stress distribution in all blade components. Those results have been reviewed and based on it, three possible layouts of spar proposed. Simultaneously, resulting stress distribution after modifications were calculated and checked. There were some locations of high stress concentrations, however, they were very small (of single element size). Therefore, it was decided it can be neglected as this situation cannot occur in real.

The numerical calculations described herein allowed estimating weight and costs reductions of the propeller. It is possible to reduce the total propeller weight by 6% and although it does not seem much, it is still worth addressing. The reduction of materials used gives an opportunity to reduce the total cost of a single propeller up to 30%, however, it should be precisely analyzed before any changes to its documentation are introduced and the first units made. The current structure should be further investigated and improved, for example, chamfering of layers could be implemented to avoid stress concentrations and reduce the weight further.

REFERENCES

[1] Zasuwa, M., 2013, "Oblot motoszybowca z napędem elektrycznym AOS-71", from http://www.meil.pw.edu.pl/pl/MEiL/Aktualnosci/Ogloszenia-rozne/Oblot-motoszybowca-z-napedem-elektrycznym-AOS-71

[2] Haintze, K., 2009, "Computer Methods in Optimalization of Fiber Composites Structures", Transactions of the Institute of Aviation, 200, pp. 60-71.

[3] Lis, M., 2011, "Optymalizacja struktury konstrukcyjnej śmigła motoszybowca AOS-71", MSc thesis, Warsaw University of Technology, Warsaw, Poland.

[4] Różański, P. and Wnuk, G., 2009, "Badanie lotniczych struktur kompozytowych na przykładzie kadłuba wiatrakowca XENON", MSc thesis, Warsaw University of Technology, Warsaw, Poland.

[5] Sałacińska, A., 2016, "Przegląd wymaganych badań fizycznych do kwalifikacji materiałów kompozytowych", Transactions of the Institute of Aviation, 243, pp. 161-169.

[6] Czajkowska, K., Szeląg, D., Lorenc, Z. and Czarnocki, P., 2011, "Odporność laminatu węglowo-epoksydowego na zmęczeniowy rozwój rozwarstwień w warunkach ISP", Transactions of the Institute of Aviation, 221, pp. 18-25.

[7] Madhusudhan, B.M. and Srihari, P.V., 2014, "Design and Analysis of Composite propeller Blade for Aircraft", Journal of Engineering Research and Applications, 4(9), pp. 79-82.

[8] Goraj, Z., 2007, "Load Composite Structure in Aeronautical Engineering", Transactions of the Institute of Aviation, 191, pp. 13-32.

[9] Jaiganesh, V., Manivannan, S. and Manivannan, S., 2014, "Numerical Analysis and Simulation of Nylon Composite Propeller for Aircraft", Proceedings of the 12th Global Congress on Manufacturing and Management, Vol. 97, Vellore, India, pp. 1079-1088.

[10] Bochenek, M., 2010, „Projekt wstępny i obliczenia śmigła kompozytowego", MSc thesis, Warsaw University of Technology, Warsaw, Poland.

[11] HyperMesh tutorials, 2011, from http://www.cadfamily.com/a/CAE_FEA_CFD/hyperworks/

[12] Barbero, E.J., 2008, Finite element analysis of composite materials, 1st ed., CRC Press/Taylor & Francis Group, New York, NY.

[13] Moaveni, S., 1999, Finite element Analysis. Theory and Application with ANSYS, 1st ed., Prentice Hall, New York, NY.

[14] Jasiński, D., 2011, "Analiza numeryczna opływu śmigła motoszybowca AOS-71", Report not published, Warsaw University of Technology, Warsaw, Poland.

[15] Romander, E.A. and Field, M., 2002, "Computational simulation of propellers in cruise", Proceedings of the 23rd Congress of International Council of the Aeronautical Sciences, Toronto, Canada.

[16] Nagpurwala, Q.H., Subbaramu, M.D., Deshpande, M.D. and Shankapal, S.R, 2014, "Parametric studies on the Aerodynamic Performance of a Miniature Propeller for MAV Application", Proceedings of the 16th CFD Annual symposium, Bangalore, India.

[17] Woelke, M., 2007, "Eddy Viscosity Turbulence Models Employed by Computational Fluid Dynamic", Transactions of the Institute of Aviation, 191, pp. 92-113.

[18] Szafran, K., Shcherbonos, O. and Ejmocki, D., 2014, "Effects of Duct Shape on Ducted Propeller Thrust Performance", Transactions of the Institute of Aviation, 237, pp. 84-91.
[19] Wiśniowski, W., 2010, "Badania rezonansowe obiektów latających - metody i analiza wyników", Transactions of the Institute of Aviation, 209.
[20] Parafiniak, M. and Skalski, P., 2011, "Vibration Testing of a Helicopter Main Rotor Composite Blade", Transactions of the Institute of Aviation, 218, pp. 72-76.
[21] ANSYS tutorials, 2011, from http://www.mece.ualberta.ca/tutorials/ansys/index.html
[22] Havel Composites shop website, 2011, from http://www.havel-composites.com

NUMERYCZNA ANALIZA I OPTYMALIZACJA STRUKTURY ŚMIGŁA MOTOSZYBOWCA

Streszczenie

Celem artykułu jest przedstawienie metodologii analizy numerycznej i optymalizacji struktury śmigła kompozytowego wchodzącego w skład zespołu napędowego motoszybowca AOS-71. Głównym celem jest minimalizacja masy śmigła, co jest zawsze pożądane w lotnictwie oraz redukcja zużycia materiałów konstrukcyjnych, co z kolei przekłada się na koszt wytworzenia śmigła. Na wstępie pokazano ogólne informacje odnośnie wymagań, jakim powinno sprostać badane śmigło. Następnie przedstawiono ogólne dane techniczne i warunki pracy śmigła. W dalszej kolejności opisane są kolejne etapy analizy prowadzące do finalnych wyników. Składa się na nie utworzenie modelu trójwymiarowego dla przyjętych założeń na temat geometrii, budowa siatki elementów skończonych, która możliwie dokładnie odwzorowuje rzeczywisty obiekt oraz przygotowania i analizy z wykorzystaniem program ANSYS. Finalnym wynikiem przedstawionym w artykule są rezultaty analizy oraz ocena metodologii i wnioski do projektowania przyszłych konstrukcji śmigieł.
Słowa kluczowe: optymalizacja numeryczna, struktury kompozytowe, MES, śmigło motoszybowca.